Using satellite observations to evaluate model representation of Arctic mixed-phase clouds

J. Shaw[1*], Z. S. McGraw[1†], O. Bruno[2], T. Storelvmo[1,3], and S. Hofer[1]

[1]Department of Geosciences, University of Oslo, Oslo, Norway
[2]Karlsruhe Institute of Technology, Institute of Meteorology and Climate Research
[3]School of Business, Nord University, Bodø, Norway

Key Points:

- CAM6-Oslo and CAM6 capture the vertical structure of Arctic mixed-phase clouds, with supercooled liquid cloud tops overlying icy interiors.
- Removing an error in CAM6 that limits heterogeneous nucleation processes and ice number reduces supercooled liquid water in Arctic clouds.
- Modelled present-day winter and spring cloud fraction can predict Arctic longwave cloud feedbacks under a +4K warming scenario.

*Now at Department of Atmospheric and Oceanic Sciences, University of Colorado at Boulder
†Now at Department of Applied Physics and Applied Mathematics, Columbia University

Corresponding author: Jonah Shaw, jonah.shaw@colorado.edu

Abstract

Clouds play an important role in determining Arctic warming, but remain difficult to constrain with available observations. We use two satellite-derived cloud phase metrics to investigate the vertical structure of Arctic clouds in global climate models that use the Community Atmosphere Model version 6 (CAM6) atmospheric component. We produce a set of constrained model runs by adjusting model microphysical variables to match the cloud phase metrics. Models in this small ensemble have variable representation of cloud amount and phase in the winter, while uniformly underestimating total cloud cover in the spring and overestimating it in the summer. We find a consistent correlation between winter and spring cloud cover simulated for the present-day and the longwave cloud feedback parameter.

Plain Language Summary

[Clouds are important regulators of warming in the Arctic. The thermodynamic phase of a cloud affects its lifetime and transparency to incoming and outgoing radiation. As a result, transitions from ice to liquid in a warming climate change the influence of clouds on surface temperature. At temperatures between −37 °C and 0 °C, both ice and supercooled liquid water may exist simultaneously in a cloud layer. Global climate models struggle to capture cloud phase in this temperature range because it depends on both cloud temperature and aerosol properties. This study investigates how the fraction of supercooled liquid water changes vertically in Arctic clouds, comparing liquid-rich cloud tops with their icy interiors. We describe a model error that limits the formation of new ice crystals. We also find that global climate models reproduce observations, and can be tuned to achieve better agreement by adjusting two model parameters. Changes in cloud cover resulting from these adjustments mostly occur in the winter and spring, and cause the models to trap longwave radiation differently. The results of this study highlight the need to capture seasonal changes in cloud phase and amount in order to successfully predict future changes to the Arctic climate.]

1 Introduction

Uncertainties in cloud and aerosol radiative effects are a principal contributor to climate model uncertainty, and remain so despite decades of research and model development (Boucher et al., 2013). These uncertainties arise from the difficulty of representing aerosol-cloud interactions and other key physical processes at the typical resolutions of global climate models (GCMs). Evaluations of available models from the Coupled Model Intercomparison Project Phase 6 (CMIP6) (Eyring et al., 2016; Taylor et al., 2012) indicate that changes in climate sensitivity relative to CMIP5 are mostly due to changes in cloud representation, specifically for extratropical low-level clouds (Zelinka et al., 2020) Using observations to reevaluate the representation of these clouds in the latest generation of GCMs is a vital part of testing the validity of these new predictions.

In the Arctic, clouds mediate climate change through interactions with land and sea ice, and impacts on surface radiative fluxes (H. Morrison et al., 2012). As the thermodynamic phase of Arctic clouds shifts from ice to liquid while clouds respond to warming, the radiative effect that they exert on the surface changes (Mitchell et al., 1989). This process, known as the cloud phase feedback, depends on cloud optical thickness and lifetime changes. The magnitude and sign of the cloud phase feedback is dependent on initial cloud state, the underlying surface type, and the presence of aerosols active as cloud condensation nuclei and ice nucleating particles (INPs). In the Arctic, the amount of longwave warming resulting from the cloud phase feedback is highly sensitive to model microphysical changes (Tan & Storelvmo, 2019).

At temperatures between approximately −37 °C and 0 °C, cloud ice forms via heterogeneous nucleation processes that are dependent on temperature, in-cloud vapor pressure, and the presence of INPs (Korolev, 2007). Ice, liquid, and mixed-phase clouds can coexist in this regime. The fraction of supercooled liquid water in a mixed-phase cloud layer can be referred to as the supercooled liquid fraction (SLF) (Komurcu et al., 2014). Despite the thermodynamically unstable nature of co-suspended ice crystals and liquid droplets, observations show that Arctic mixed-phase clouds are both common and long-lived (Matus & L'Ecuyer, 2017; H. Morrison et al., 2012). This longevity is due in part to the vertical structure of Arctic mixed-phase clouds. These clouds are roughly partitioned into INP-limited liquid cloud tops and glaciated interiors, preventing ice from quickly depleting cloud water (Hobbs & Rangno, 1998). High-resolution modelling studies of Arctic mixed-phase clouds indicate that cloud phase is highly sensitive to ice formation mechanisms and the availability of INPs (Jiang et al., 2000; Fridlind et al., 2007; Fu et al., 2019). Because of their global coverage and continuous record, satellite cloud retrievals are commonly used to constrain and evaluate GCM performance. The macroscopic cloud properties retrieved by satellites, however, cannot uniquely determine cloud microphysical properties or feedbacks. Additional constraints are needed to ensure that GCMs capture the climate-relevant behavior of clouds.

Observations of cloud amount and phase obtained from the Cloud-Aerosol Lidar with Orthogonal Polarization (CALIOP) sensor aboard the CALIPSO platform provide a strong observational constraint for assessing cloud representation in GCMs (Winker et al., 2009). Cloud phase is especially important, as observations of cloud amount alone may hide compensating phase biases with large radiative impacts (Cesana & Chepfer, 2012; Cesana et al., 2012). Comparing CMIP5-era GCMs against CALIOP cloud phase retrievals revealed a consistent underestimation of cloud liquid water content at mixed-phase temperatures, corresponding to insufficient cloud liquid and excess cloud ice (Komurcu et al., 2014). The reduction of this bias is largely responsible for increases in climate sensitivity in CMIP6 (Zelinka et al., 2020). In the Arctic, both CMIP5 models and reanalysis data products struggle to reproduce observed cloud phase and optical depth (Lenaerts et al., 2017). Tan and Storelvmo (2019) found that minimizing global cloud phase biases in the CESM1 model yielded a broad range of cloud microphysical variables and Arctic Amplification factors. Our model simulations continue this work with CAM6, a CMIP6-era atmospheric model, focusing model adjustments and analysis on the Arctic and assessing model performance with additional observational constraints.

Version 6 of the Community Atmosphere Model (CAM6) is the most recent version of CAM, and is used in several CMIP6-era models. The Cloud Feedback Model Intercomparison Project (CFMIP) Observational Simulator Package: Version 2 (COSP2) is integrated into CAM6, enabling scale- and definition-aware comparisons against satellite products like those produce by CALIOP (Swales et al., 2018). Important changes to CAM6 relative to CAM5 include a separate ice nucleation scheme for heterogeneous freezing (Hoose et al., 2008) and an updated microphysics scheme for stratiform clouds (H. Morrison & Gettelman, 2008). Sensitivity studies with CESM2 show that the addition of these new components cause significant changes to precipitation and cloud cover over the Greenland Ice Sheet, motivating further investigation of cloud representation over the entire Arctic region (Lenaerts et al., 2020).

2 Methods

2.1 Cloud Phase Metrics

Measurements of cloud phase were retrieved from NASAs Cloud-Aerosol Lidar with Orthogonal Polarization (CALIOP) instrument (Winker et al., 2009) for a four year observational period from 1 June 2009 through 31 May 2013. SLF is calculated following the procedures described in Bruno et al. (2021) and is represented on isotherms from -

40°C to 0°C, with a 5°C increment. To investigate the vertical structure of mixed-phase clouds, we filter by overlying cloud optical thickness (COT) to produce two SLF metrics. We obtain one metric (hereafter: cloud-top SLF) by selecting only the highest layer of observed mixed-phase clouds after discarding the uppermost layers with COT < 0.3 in order to avoid including optically-thin cirrus clouds. Another metric (hereafter: cloud-bulk SLF) is obtained by selecting all cloud layers retrieved by CALIOP with overlying COT less than 3.0. The same COT filters are applied when producing comparable model output from the GCMs.

2.2 Additional Satellite Products

To conduct further model evaluation of cloud amount and radiative fluxes, we compare against the GCM–Oriented CALIPSO Cloud Product (GOCCP) Version 3 (Chepfer et al., 2010) and Clouds and the Earths Radiant Energy System Energy Balanced and Filled (CERES-EBAF) Ed4.0 datasets (Kato et al., 01 Jun. 2018). The GOCCP data product separates total cloud cover into liquid, ice, and undefined phases, and is produced specifically for comparison with the COSP satellite simulator. From CERES-EBAF, we use computed surface long- and shortwave cloud radiative effect (CRE) values and surface all-sky downwelling fluxes.

2.3 Modeling Simulations

We present atmosphere-only runs of the Nordic Earth System Model Version 2 (NorESM2) and the Community Earth System Model Version 2 (CESM2) (Seland et al., 2020; Danabasoglu et al., 2020). In order to provide a consistent comparison with the development branch of NorESM2 used, we use the 2.1.0 release of CESM2. Both models have 32 vertical levels and are run at $1.9° \times 2.5°$ horizontal resolution. We use identical model components in both GCMs to isolate the impact of differences between the atmospheric modules. Both models use CAM6, with NorESM2 implementing an alternate aerosol scheme and parametrizing mid- and high-level ice clouds differently. Runs of NorESM2 and CESM2 are subsequently referred to as CAM6-Oslo and CAM6. All modelled data represent averages over the same 4-year period from which SLF values were calculated. Models are run for 3 months preceding this period to allow the atmosphere to adjust to microphysics changes. To reduce variability in meteorology between runs, we nudge horizontal winds and surface pressure to ERA-Interim reanalysis data for the observational period (Dee et al., 2011). Finally, we enable COSP2 in order to produce additional cloud variables for comparison with CALIOP cloud products.

2.4 Model Modifications

INP availability is an important limiting factor in cloud glaciation at mixed-phase temperatures. In CAM6 and CAM6-Oslo, the in-cloud ice number concentration cannot exceed the calculated concentration of available ice nuclei. The new heterogeneous nucleation processes in CAM6 do not contribute to this INP limit, preventing them from nucleating ice crystals. Heterogeneous nucleation processes are still able to increase ice crystal mass, however, and can artificially inflate ice crystal size and increase sedimentation. This model error has been shared with model developers and flagged as an issue to be resolved in future releases of CAM (personal communications, A. Gettelman, 2021) (Gettelman, 2021).

To assess the importance of this model mechanism on cloud properties and ice number concentration and size, we disable the ice number limit at mixed-phase temperatures ($-37°\text{C} < T < 0°\text{C}$) in CAM6-Oslo, producing an additional model variation that we label as CAM6-OsloIce. We also limit the rate of secondary ice production in CAM6-OsloIce to avoid strong secondary production in the absence of the ice number limit. To focus on Arctic clouds, these changes are made only in the Arctic Circle (latitude $> 66°$

Run name	Model	Ice Number Limit	WBF Multiplier	INP Multiplier	Average Ice Radius at 860 hPa (um)	Ice Concentration at 860 hPa (m-3)
CAM6-Oslo	NorESM2	Yes	1.0	1.0	151	4120
CAM6	CESM2	Yes	1.0	1.0	165	5550
CAM6-OsloIce	NorESM2	No	1.0	1.0	132	15670
CAM6-Oslo Fit 1	NorESM2	Yes	1.25	10.0	163	3870
CAM6-OsloIce Fit 2	NorESM2	No	0.5	0.05	124	5410
CAM6-OsloIce Fit 3	NorESM2	No	0.2	0.1	112	8600
CAM6 Fit 4	CESM2	Yes	1.0	100	209	5060

Table 1. Model run descriptions.

N). Whereas mixed-phase clouds in CAM6 are strongly (and potentially unrealistically) INP-limited by the ice number limit, CAM6-OsloIce serves as an alternate ensemble end-member for which the availability of INPs is effectively removed as a limiting factor in the glaciation of mixed-phase clouds.

Tan and Storelvmo (2016) identified the Wegener–Bergeron–Findeisen (WBF) time scale and the number of dust aerosols active as INPs as the most important variables for cloud phase partitioning in CAM5. We modify these two variables in the base models (CAM6-Oslo, CAM6, and CAM6-OsloIce) to reduce the root-mean-square error in both SLF metrics concurrently, producing four "fitted" GCM simulations. Parameter modifications are chosen to give the best model-observation agreement, and to create a range of microphysical cloud representations. Table 1 summarizes the six GCM simulations presented in this work with selected microphysics variables.

2.5 Radiative Feedback Calculations

We use surface radiative kernels from Soden et al. (2008) to calculate long- and shortwave cloud feedback parameters. We repeat each standard and fitted model run with the prescribed sea surface temperatures increased by 4K to create perturbed runs for the radiative feedback calculations. Because we run atmosphere-only simulations and modify models only poleward of 66°N, feedback parameters are calculated with respect to the temperature change in the Arctic rather than the global mean. Results are qualitatively similar to feedback parameters normalized to globally-averaged temperature changes.

3 Results

3.1 SLF Metrics

Figure 1(a) shows the SLF metrics from CALIOP observations and the base models. In the CALIOP retrievals, cloud-top SLF is greater than cloud-bulk SLF values for all isotherms between −35°C and −10°C. At −20°C where this difference is the most pronounced, cloud-top SLF exceeds the cloud-bulk value by nearly a factor of three. This vertical structure of optically-thick cloud tops indicates the importance of cloud tops as both a source of INPs and a barrier to efficient radiative cooling in the interior of clouds. All models reproduce the structure of icier cloud interiors, but with varying degrees of quantitative agreement with CALIOP. CAM6-Oslo shows strong agreement across both metrics, CAM6 overestimates SLF in cloud tops, and CAM6-OsloIce underestimates SLF along both the cloud-top and cloud-bulk SLF metrics. The poor performance of CAM6-OsloIce results from a high ice number concentration that allows liquid water to be quickly depleted. This result indicates that INP-limited environments are necessary for main-

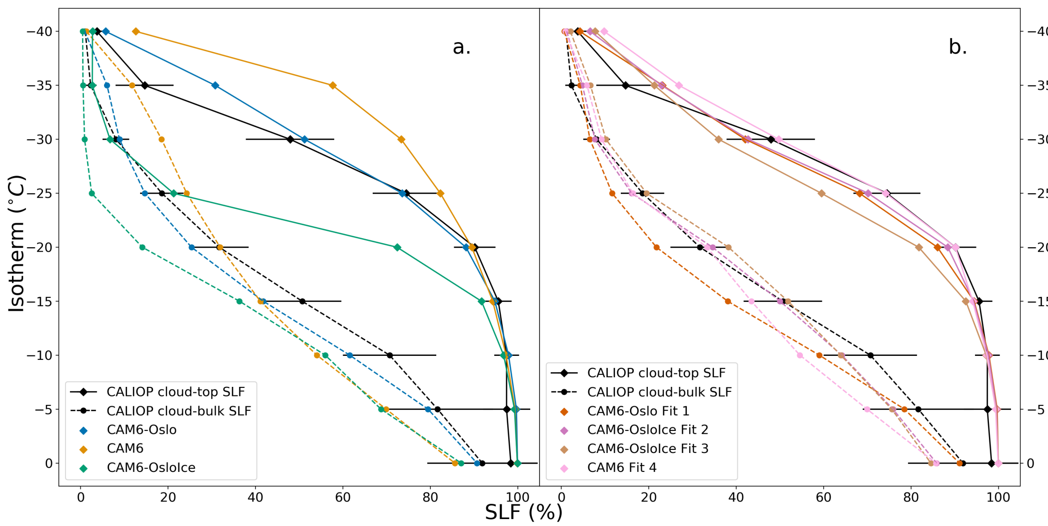

Figure 1. Supercooled liquid fraction by isotherm for cloud-top and cloud-bulk metrics for (a) base models and (b) fitted models. Error bars on CALIOP SLF values correspond to one standard deviation. All values represent the average from 66°-82°N.

taining liquid cloud tops below −20°C. However, these results do not uniquely determine the source of excess ice.

Figure 1(b) shows SLF metrics for CALIOP and the fitted models. Strong agreement with CALIOP indicates that adjusting only two model parameters can effectively tune SLF values across both metrics at the same time. Ice crystal size and concentration variables in the constrained runs (Table 1) vary by roughly a factor of two even when matching both SLF metrics, indicating that these observations do not provide a strong constraint on the ice crystal properties. Runs without an ice number limit have smaller ice crystals and higher concentrations than those with the limit in place. Comparing CAM6 and CAM6 Fit 4 in Table 1 demonstrates the model error discussed in Section 2.4: Raising INP concentrations in the heterogeneous nucleation scheme increases ice mass but not ice crystal number, causing ice crystals grow larger and sediment more quickly.

3.2 Evaluation against CALIOP-GOCCP and CERES-EBAF data products

Monthly averages of cloud amount by CALIOP phase designation allow us to identify seasonal trends and biases (Figure 2). We find that fitting to the SLF metrics brings CAM6-Oslo and CAM6-OsloIce models into good agreement, indicating that the effect of removing the limit on ice number can be compensated for with the adjustment of the WBF and INP parameters. In the summer and early fall, the total cloud fraction and the liquid and ice components are consistent across all models, with an overestimation of liquid and total cloud fraction during June and July. Differences between models emerge in the winter and spring months. CAM6-OsloIce, CAM6-Oslo Fit 1, CAM6-Oslo Fit 2, and CAM6 Fit 4 all produce insufficient total cloud fraction during the winter, while CAM6 produces excess total cloud fraction. All models fail to capture the total cloud fraction in the spring, mostly due to insufficient ice cloud fraction. Finally, a positive liquid cloud bias in CAM6 persists throughout the year and is especially pronounced during the winter.

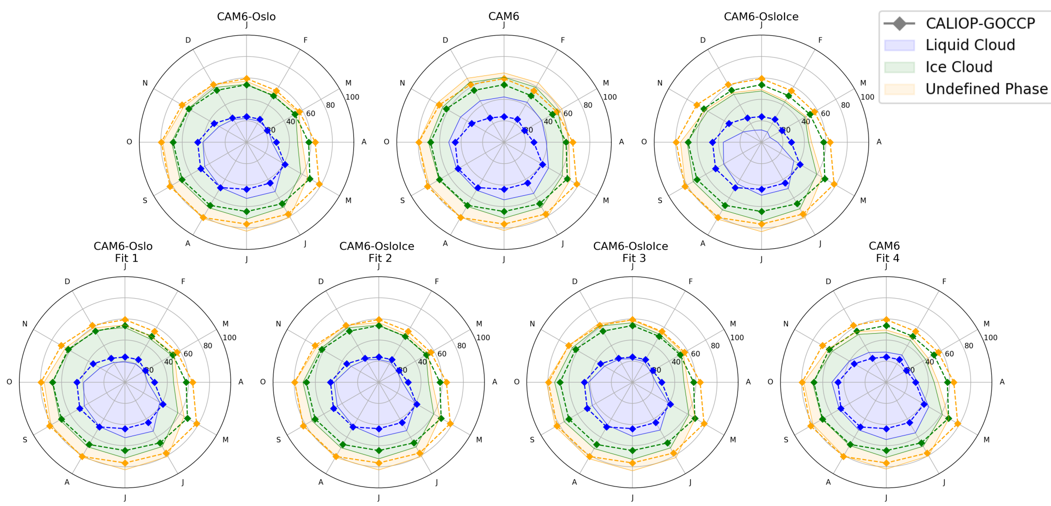

Figure 2. Monthly averages of cloud fraction by CALIOP phase designation for all model simulations. Cloud of undefined phase is included so that the total cloud fraction can be visualized and compared between models.

Annual model biases in Arctic-averaged cloud fraction and CRE with respect to CALIOP-GOCCP and CERES-EBAF (Table S1) follow the results of Figure 2. Notable compensating biases in cloud amount by phase are present, with CAM6 producing excess liquid cloud and insufficient ice cloud, and CAM6-OsloIce producing excess ice cloud and insufficient liquid cloud. CAM6 Fit 4 shares the ice cloud bias of CAM6 despite having good agreement with the observed SLF metrics because positive biases in mid- and high-level ice clouds are unaffected by the model adjustments. Despite differences in the annual-average cloud representation by phase across the models, annual shortwave CRE biases are all negative. Polar projections of model cloud phase biases (Figure S1) show the spatial features of model cloud phase biases.

Downwelling shortwave surface flux and CRE biases (Fig. 3(a) and (b)) strongly resemble each other, indicating that clouds are responsible for the shortwave biases. Excess summer cloud fraction increases shortwave reflection and produces the negative shortwave CRE biases in Table S1. We expect that this excessive cloudiness is largely unrelated to cloud phase, since low-level Arctic clouds will generally have temperatures above 0°C during the summer months. This explanation is supported by the weak model sensitivity to aerosol and cloud microphysics changes during this time.

Like the shortwave, the downwelling longwave surface flux and CRE biases (Fig. 3(c) and (d)) are also highly similar. There is strong seasonal variation in the longwave biases, with excess downward flux from clouds in the summer and insufficient downward flux in the winter. The positive summer biases occur when all models produce excess cloud fraction, but the negative wintertime biases occur even in the models that capture both cloud fraction and phase well. That CAM6, which overproduces winter cloud cover, is the only model to capture the downward flux suggests the existence of a bias in cloud height and emission temperature across all simulations. While passive sensors and their corresponding satellite simulators are poorly suited to constrain this behavior, cloud height and opacity variables recently incorporated into the COSP2 Lidar simulator will allow this wintertime bias to be investigated in future versions of CAM (Guzman et al., 2017; A. L. Morrison et al., 2019).

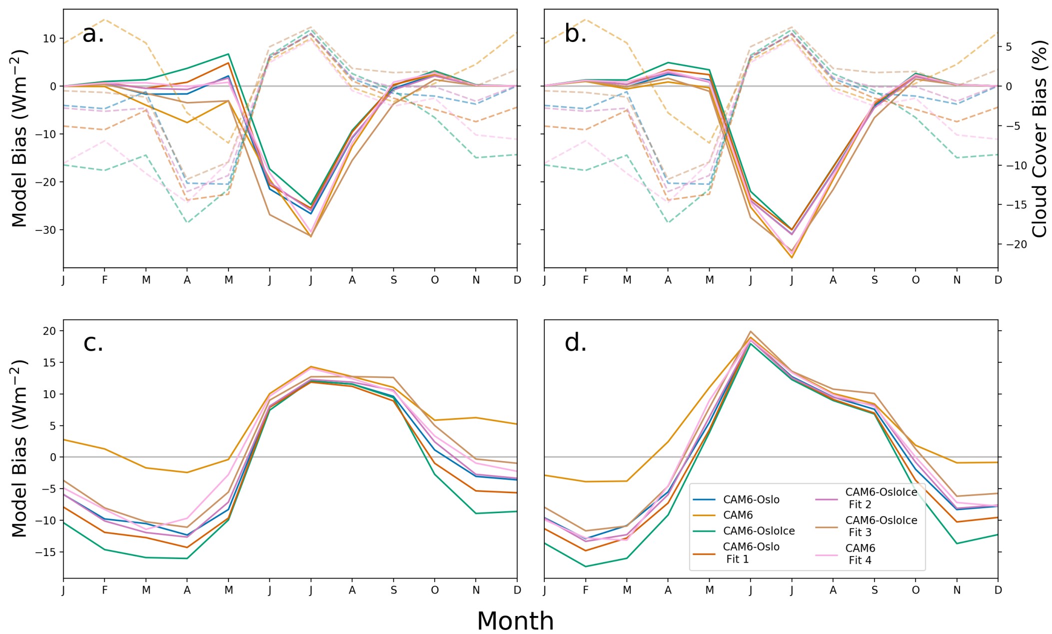

Figure 3. Monthly values for: (a) Model bias in shortwave downwelling flux at the surface (solid) and total cloud amount (dashed), (b) Model bias in surface shortwave cloud radiative effect (solid) and total cloud amount (dashed), (c) Model bias in longwave downwelling flux at the surface, (d) Model bias in surface longwave cloud radiative effect.

3.3 Cloud Radiative Feedbacks

Computing cloud radiative feedbacks allows us to assess the relative importance of the long- and shortwave cloud feedback processes and to investigate their dependence on the present-day cloud state and cloud microphysical properties. Figure 4(a) shows the long- and shortwave cloud feedback parameters and the net cloud feedback for each model simulation. Models with a greater increase in low cloud fraction (Figure 4(b)) have greater short- and longwave cloud feedbacks, since increases in cloud lifetime and optical depth associated with cloud phase changes magnify both shortwave cooling and longwave warming. Surface temperature changes (Figure 4(c)) generally mirror the net cloud feedback with the exception of CAM6.

CAM6 Fit 4 and CAM6-OsloIce Fit 3 have the greatest longwave feedbacks and also share large total cloud fraction deficits during the winter and spring (Figure 2). We hypothesize that insufficient cloud cover during these months provides a greater potential for rapid increases in low-level cloud amount under warming and large longwave cloud feedbacks. To test this hypothesis, we regress the longwave cloud feedback parameter against cloud cover bias in the present day simulations. We find that the mean cloud cover bias from November through April is well correlated with the longwave feedback ($R^2 = 0.61$) (Figure 4(d)). Individual correlations by month indicate that this pattern is consistent during the winter and spring (Figure S2). These results support our hypothesis that longwave cloud feedback could be predicted with present-day winter and spring cloud cover.

Discussion of cloud phase feedback is often limited to changes in optical depth and shortwave cloud forcing. Our results show that in the Arctic, cloud fraction changes in the winter and spring play an important role in determining the total cloud forcing via

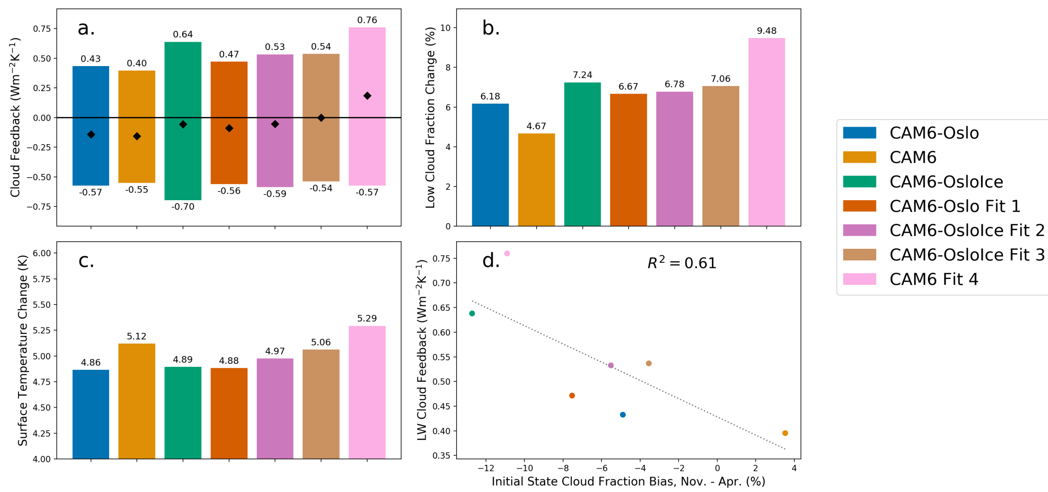

Figure 4. a. Arctic-averaged longwave and shortwave cloud feedback. Diamonds denote the net cloud feedback. Kernel calculations do not incorporate surface albedo changes with mean state when calculating shortwave cloud feedback and tend to overestimate the shortwave cooling effect of clouds at high latitudes. b. Arctic-averaged change in low cloud amount between initial and +4K simulations. c. Arctic-averaged surface temperature change. d. Longwave cloud feedback as a function of the cloud cover bias from November to April in the simulated present-day.

changes to the longwave feedback. Cloud properties in the warmer and brighter months continue to dominate the shortwave cloud feedback, but these clouds are generally liquid and thus insensitive to changes in model mixed-phase processes.

4 Discussion and Conclusion

We find large differences in thermodynamic phase between cloud tops and interiors in satellite observations of Arctic mixed-phase clouds, consistent with previous ground-based measurements. CAM6-Oslo captures this vertical phase structure better than CAM6, suggesting that model aerosol schemes and high cloud parameterizations play an important role in determining cloud phase. We evaluate a model error that prevents heterogeneous nucleation processes from creating new ice crystals and find that cloud water is significantly reduced when these nucleation processes are able to operate freely. Modifying two microphysical parameters can bring models into agreement with SLF observations even after enabling heterogeneous nucleation by removing the model limit on cloud ice crystal number. The need to understand the relative importance of different ice sources (heterogeneous nucleation, sedimentation, detrainment) in low-level mixed-phase clouds, as suggested in Fridlind et al. (2007) and Klein et al. (2009), is made more apparent by these findings.

All models produce insufficient cloud fraction in the spring and excess cloud fraction in the summer. The summer bias dominates the shortwave impact, leading to a net negative annual shortwave flux bias. The longwave flux bias is strongly seasonal, with a positive summer bias explained by excess summer cloud fraction and a negative winter bias likely resulting from low-biased cloud emission temperatures. We note that constraining models to the SLF metrics with the model adjustments employed here only corrects biases at mixed-phase temperatures, leaving biases in low-level liquid clouds and high-level ice clouds unchanged. This effect is demonstrated by the high similarity in cloud amount by phase across all models in the summer and early fall when warm liquid clouds are common.

The greatest variation between models occurs in the winter and spring, and cloud fraction during these seasons largely determines differences in longwave cloud radiative feedback. Models with less initial winter and spring cloud gain more cloud cover when surface temperatures are increased, leading to a greater longwave feedback. Regressing the longwave feedback against the winter and spring cloud fraction reveals a consistent negative correlation. Our ability to draw robust conclusions from this result is limited by the small number of simulations, motivating future work across multiple models to investigate whether winter and spring cloud amount can be used as an emergent constraint on Arctic cloud feedbacks.

Using Arctic data from fully-coupled simulations constrained to global SLF observations, Tan and Storelvmo (2019) found that Arctic warming was highly sensitive to changes in the rate of the WBF process and the concentration of INPs. Our atmosphere-only simulations constrained to SLF in the Arctic highlight the importance of how models handle INP availability and their ability to capture the observed cloud state. We show that the transition to higher cloud cover in the Arctic winter controls longwave cloud feedbacks. Future fully-coupled simulations under a realistic forcing scenario should explore how quickly this transition takes place and its dependence on model microphysical parameters.

Acknowledgments

This project has received funding from the European Research Council (ERC) under the European Unions Horizon 2020 research and innovation programme under grant agreement No 714062 (ERC Starting Grant C2Phase). This work was supported by the European Research Council (ERC) through Grant StG 758005, and by the Norwegian Research Council through grant 295046. The computations and simulations were performed on resources provided by UNINETT Sigma2 - the National Infrastructure for High Performance Computing and Data Storage in Norway. JKS acknowledges funding from a Fulbright Student Research Grant. JKS also thanks Anne Claire Fouilloux and Inger Helene Karset for technical support and JE Kay for comments.

CALIOP and CERES-EBAF data are available online at the NASA Langley Atmospheric Sciences Data Center website (https://asdc.larc.nasa.gov/). The CALIOP GOCCP observational data set can be downloaded from https://climserv.ipsl.polytechnique.fr/cfmip-obs/. The ERA-Interim reanalysis data can be downloaded from https://www.ecmwf.int/en/forecasts/datasets/reanal datasets/era-interim.

References

Boucher, O., Randall, D., Artaxo, P., Bretherton, C., Feingold, G., Forster, P., . . . Zhang, X. (2013). Clouds and aerosols [Book Section]. In T. Stocker et al. (Eds.), *Climate change 2013: The physical science basis. contribution of working group i to the fifth assessment report of the intergovernmental panel on climate change* (p. 571658). Cambridge, United Kingdom and New York, NY, USA: Cambridge University Press. Retrieved from `www.climatechange2013.org` doi: 10.1017/CBO9781107415324.016

Bruno, O., Hoose, C., Storelvmo, T., Coopman, Q., & Stengel, M. (2021). Exploring the cloud top phase partitioning in different cloud types using active and passive satellite sensors. *Geophysical Research Letters*, *48*(2), e2020GL089863. Retrieved from `https://agupubs.onlinelibrary.wiley.com/doi/abs/10.1029/2020GL089863` (e2020GL089863 2020GL089863) doi: https://doi.org/10.1029/2020GL089863

Cesana, G., & Chepfer, H. (2012). How well do climate models simulate cloud vertical structure? a comparison between calipso-goccp satellite observations and cmip5 models. *Geophysical Research Letters*, *39*(20). Retrieved from https://agupubs.onlinelibrary.wiley.com/doi/abs/10.1029/2012GL053153 doi: 10.1029/2012GL053153

Cesana, G., Kay, J. E., Chepfer, H., English, J. M., & de Boer, G. (2012). Ubiquitous low-level liquid-containing arctic clouds: New observations and climate model constraints from calipso-goccp. *Geophysical Research Letters*, *39*(20). Retrieved from https://agupubs.onlinelibrary.wiley.com/doi/abs/10.1029/2012GL053385 doi: 10.1029/2012GL053385

Chepfer, H., Bony, S., Winker, D., Cesana, G., Dufresne, J. L., Minnis, P., … Zeng, S. (2010). The gcm-oriented calipso cloud product (calipso-goccp). *Journal of Geophysical Research: Atmospheres*, *115*(D4). Retrieved from https://agupubs.onlinelibrary.wiley.com/doi/abs/10.1029/2009JD012251 doi: 10.1029/2009JD012251

Danabasoglu, G., Lamarque, J.-F., Bacmeister, J., Bailey, D. A., DuVivier, A. K., Edwards, J., … Strand, W. G. (2020). The community earth system model version 2 (cesm2). *Journal of Advances in Modeling Earth Systems*, *12*(2), e2019MS001916. Retrieved from https://agupubs.onlinelibrary.wiley.com/doi/abs/10.1029/2019MS001916 (e2019MS001916 2019MS001916) doi: 10.1029/2019MS001916

Dee, D. P., Uppala, S. M., Simmons, A. J., Berrisford, P., Poli, P., Kobayashi, S., … Vitart, F. (2011). The era-interim reanalysis: configuration and performance of the data assimilation system. *Quarterly Journal of the Royal Meteorological Society*, *137*(656), 553-597. Retrieved from https://rmets.onlinelibrary.wiley.com/doi/abs/10.1002/qj.828 doi: 10.1002/qj.828

Eyring, V., Bony, S., Meehl, G. A., Senior, C. A., Stevens, B., Stouffer, R. J., & Taylor, K. E. (2016). Overview of the coupled model intercomparison project phase 6 (cmip6) experimental design and organization. *Geoscientific Model Development*, *9*(5), 1937–1958. Retrieved from https://www.geosci-model-dev.net/9/1937/2016/ doi: 10.5194/gmd-9-1937-2016

Fridlind, A. M., Ackerman, A. S., McFarquhar, G., Zhang, G., Poellot, M. R., DeMott, P. J., … Heymsfield, A. J. (2007). Ice properties of single-layer stratocumulus during the mixed-phase arctic cloud experiment: 2. model results. *Journal of Geophysical Research: Atmospheres*, *112*(D24). Retrieved from https://agupubs.onlinelibrary.wiley.com/doi/abs/10.1029/2007JD008646 doi: 10.1029/2007JD008646

Fu, S., Deng, X., Shupe, M. D., & Xue, H. (2019). A modelling study of the continuous ice formation in an autumnal arctic mixed-phase cloud case. *Atmospheric Research*, *228*, 77 - 85. Retrieved from http://www.sciencedirect.com/science/article/pii/S0169809518313905 doi: https://doi.org/10.1016/j.atmosres.2019.05.021

Gettelman, A. (2021). *Issue 20 escomp/pumas.* https://github.com/ESCOMP/PUMAS/issues/20. GitHub.

Guzman, R., Chepfer, H., Noel, V., Vaillant de Gulis, T., Kay, J. E., Raberanto, P., … Winker, D. M. (2017). Direct atmosphere opacity observations from calipso provide new constraints on cloud-radiation interactions. *Journal of Geophysical Research: Atmospheres*, *122*(2), 1066-1085. Retrieved from https://agupubs.onlinelibrary.wiley.com/doi/abs/10.1002/2016JD025946 doi: https://doi.org/10.1002/2016JD025946

Hobbs, P. V., & Rangno, A. L. (1998). Microstructures of low and middle-level clouds over the beaufort sea. *Quarterly Journal of the Royal Meteorological Society*, *124*(550), 2035-2071. Retrieved from https://rmets.onlinelibrary.wiley.com/doi/abs/10.1002/qj.49712455012 doi:

10.1002/qj.49712455012

Hoose, C., Lohmann, U., Bennartz, R., Croft, B., & Lesins, G. (2008). Global simulations of aerosol processing in clouds. *Atmospheric Chemistry and Physics*, *8*(23), 6939–6963. Retrieved from https://www.atmos-chem-phys.net/8/6939/2008/ doi: 10.5194/acp-8-6939-2008

Jiang, H., Cotton, W. R., Pinto, J. O., Curry, J. A., & Weissbluth, M. J. (2000). Cloud resolving simulations of mixed-phase arctic stratus observed during base: Sensitivity to concentration of ice crystals and large-scale heat and moisture advection. *Journal of the Atmospheric Sciences*, *57*(13), 2105-2117. Retrieved from https://doi.org/10.1175/1520-0469(2000)057<2105:CRSOMP>2.0.CO;2 doi: 10.1175/1520-0469(2000)057⟨2105:CRSOMP⟩2.0.CO;2

Kato, S., Rose, F. G., Rutan, D. A., Thorsen, T. J., Loeb, N. G., Doelling, D. R., … Ham, S.-H. (01 Jun. 2018). Surface irradiances of edition 4.0 clouds and the earths radiant energy system (ceres) energy balanced and filled (ebaf) data product. *Journal of Climate*, *31*(11), 4501 - 4527. Retrieved from https://journals.ametsoc.org/view/journals/clim/31/11/jcli-d-17-0523.1.xml doi: 10.1175/JCLI-D-17-0523.1

Klein, S. A., McCoy, R. B., Morrison, H., Ackerman, A. S., Avramov, A., Boer, G. d., … Zhang, G. (2009). Intercomparison of model simulations of mixed-phase clouds observed during the arm mixed-phase arctic cloud experiment. i: single-layer cloud. *Quarterly Journal of the Royal Meteorological Society*, *135*(641), 979-1002. Retrieved from https://rmets.onlinelibrary.wiley.com/doi/abs/10.1002/qj.416 doi: https://doi.org/10.1002/qj.416

Komurcu, M., Storelvmo, T., Tan, I., Lohmann, U., Yun, Y., Penner, J. E., … Takemura, T. (2014). Intercomparison of the cloud water phase among global climate models. *Journal of Geophysical Research: Atmospheres*, *119*(6), 3372-3400. Retrieved from https://agupubs.onlinelibrary.wiley.com/doi/abs/10.1002/2013JD021119 doi: 10.1002/2013JD021119

Korolev, A. (2007). Limitations of the wegenerbergeronfindeisen mechanism in the evolution of mixed-phase clouds. *Journal of the Atmospheric Sciences*, *64*(9), 3372-3375. Retrieved from https://doi.org/10.1175/JAS4035.1 doi: 10.1175/JAS4035.1

Lenaerts, J. T. M., Gettelman, A., Van Tricht, K., van Kampenhout, L., & Miller, N. B. (2020). Impact of cloud physics on the greenland ice sheet near-surface climate: A study with the community atmosphere model. *Journal of Geophysical Research: Atmospheres*, *125*(7), e2019JD031470. Retrieved from https://agupubs.onlinelibrary.wiley.com/doi/abs/10.1029/2019JD031470 (e2019JD031470 10.1029/2019JD031470) doi: 10.1029/2019JD031470

Lenaerts, J. T. M., Van Tricht, K., Lhermitte, S., & L'Ecuyer, T. S. (2017). Polar clouds and radiation in satellite observations, reanalyses, and climate models. *Geophysical Research Letters*, *44*(7), 3355-3364. Retrieved from https://agupubs.onlinelibrary.wiley.com/doi/abs/10.1002/2016GL072242 doi: https://doi.org/10.1002/2016GL072242

Matus, A. V., & L'Ecuyer, T. S. (2017). The role of cloud phase in earth's radiation budget. *Journal of Geophysical Research: Atmospheres*, *122*(5), 2559-2578. Retrieved from https://agupubs.onlinelibrary.wiley.com/doi/abs/10.1002/2016JD025951 doi: 10.1002/2016JD025951

Mitchell, J. F. B., Senior, C. A., & Ingram, W. J. (1989, Sep 01). C02 and climate: a missing feedback? *Nature*, *341*(6238), 132-134. Retrieved from https://doi.org/10.1038/341132a0 doi: 10.1038/341132a0

Morrison, A. L., Kay, J. E., Frey, W. R., Chepfer, H., & Guzman, R. (2019). Cloud response to arctic sea ice loss and implications for future feedback in the cesm1 climate model. *Journal of Geophysical Research: Atmospheres*, *124*(2), 1003-1020. Retrieved from https://agupubs.onlinelibrary.wiley.com/doi/abs/10.1029/2018JD029142 doi: https://doi.org/10.1029/2018JD029142

Morrison, H., de Boer, G., Feingold, G., Harrington, J., Shupe, M. D., & Sulia, K. (2012). Resilience of persistent arctic mixed-phase clouds. *Nature Geoscience*, *5*(1), 11-17. Retrieved from https://doi.org/10.1038/ngeo1332 doi: 10.1038/ngeo1332

Morrison, H., & Gettelman, A. (2008). A new two-moment bulk stratiform cloud microphysics scheme in the community atmosphere model, version 3 (cam3). part i: Description and numerical tests. *Journal of Climate*, *21*(15), 3642-3659. Retrieved from https://doi.org/10.1175/2008JCLI2105.1 doi: 10.1175/2008JCLI2105.1

Seland, Ø., Bentsen, M., Seland Graff, L., Olivié, D., Toniazzo, T., Gjermundsen, A., … Schulz, M. (2020). The norwegian earth system model, noresm2 – evaluation of thecmip6 deck and historical simulations. *Geoscientific Model Development Discussions*, *2020*, 1–68. Retrieved from https://www.geosci-model-dev-discuss.net/gmd-2019-378/ doi: 10.5194/gmd-2019-378

Soden, B. J., Held, I. M., Colman, R., Shell, K. M., Kiehl, J. T., & Shields, C. A. (2008). Quantifying climate feedbacks using radiative kernels. *Journal of Climate*, *21*(14), 3504 - 3520. Retrieved from https://journals.ametsoc.org/view/journals/clim/21/14/2007jcli2110.1.xml doi: 10.1175/2007JCLI2110.1

Swales, D. J., Pincus, R., & Bodas-Salcedo, A. (2018). The cloud feedback model intercomparison project observational simulator package: Version 2. *Geoscientific Model Development*, *11*(1), 77–81. Retrieved from https://www.geosci-model-dev.net/11/77/2018/ doi: 10.5194/gmd-11-77-2018

Tan, I., & Storelvmo, T. (2016). Sensitivity study on the influence of cloud microphysical parameters on mixed-phase cloud thermodynamic phase partitioning in cam5. *Journal of the Atmospheric Sciences*, *73*(2), 709-728. Retrieved from https://doi.org/10.1175/JAS-D-15-0152.1 doi: 10.1175/JAS-D-15-0152.1

Tan, I., & Storelvmo, T. (2019). Evidence of strong contributions from mixed-phase clouds to arctic climate change. *Geophysical Research Letters*, *46*(5), 2894-2902. Retrieved from https://agupubs.onlinelibrary.wiley.com/doi/abs/10.1029/2018GL081871 doi: 10.1029/2018GL081871

Taylor, K. E., Stouffer, R. J., & Meehl, G. A. (2012). An overview of cmip5 and the experiment design. *Bulletin of the American Meteorological Society*, *93*(4), 485-498. Retrieved from https://doi.org/10.1175/BAMS-D-11-00094.1 doi: 10.1175/BAMS-D-11-00094.1

Winker, D. M., Vaughan, M. A., Omar, A., Hu, Y., Powell, K. A., Liu, Z., … Young, S. A. (2009). Overview of the calipso mission and caliop data processing algorithms. *Journal of Atmospheric and Oceanic Technology*, *26*(11), 2310-2323. Retrieved from https://doi.org/10.1175/2009JTECHA1281.1 doi: 10.1175/2009JTECHA1281.1

Zelinka, M. D., Myers, T. A., McCoy, D. T., Po-Chedley, S., Caldwell, P. M., Ceppi, P., … Taylor, K. E. (2020). Causes of higher climate sensitivity in cmip6 models. *Geophysical Research Letters*, *47*(1), e2019GL085782. Retrieved from https://agupubs.onlinelibrary.wiley.com/doi/abs/10.1029/2019GL085782 (e2019GL085782 10.1029/2019GL085782) doi: 10.1029/2019GL085782

Figure 1.

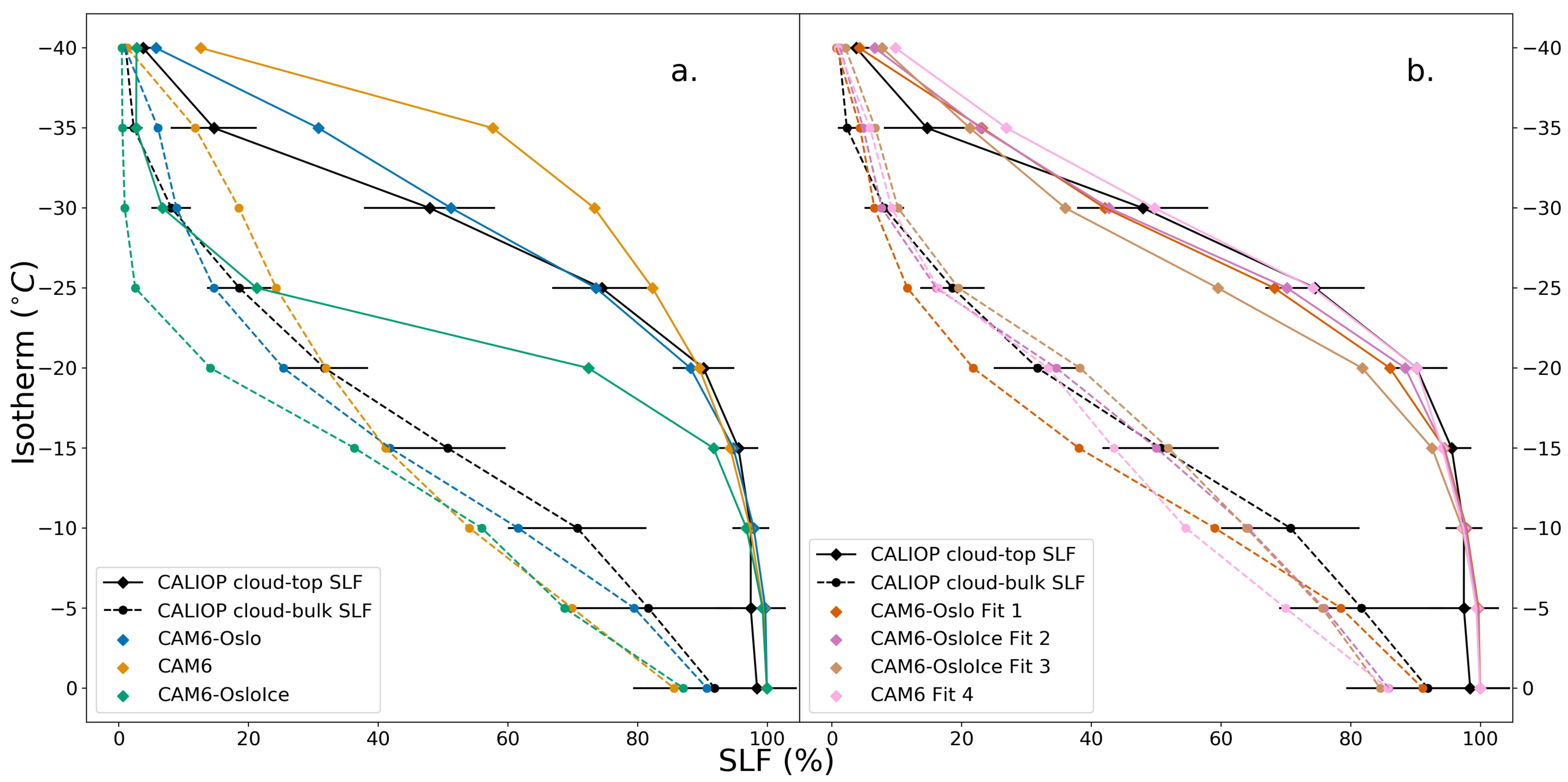

a.
b.
Isotherm (°C)
SLF (%)
−40
−35
−30
−25
−20
−15
−10
−5
0
0
20
40
60
80
100
CALIOP cloud-top SLF
CALIOP cloud-bulk SLF
CAM6-Oslo
CAM6
CAM6-OsloIce
CAM6-Oslo Fit 1
CAM6-OsloIce Fit 2
CAM6-OsloIce Fit 3
CAM6 Fit 4

Figure 2.

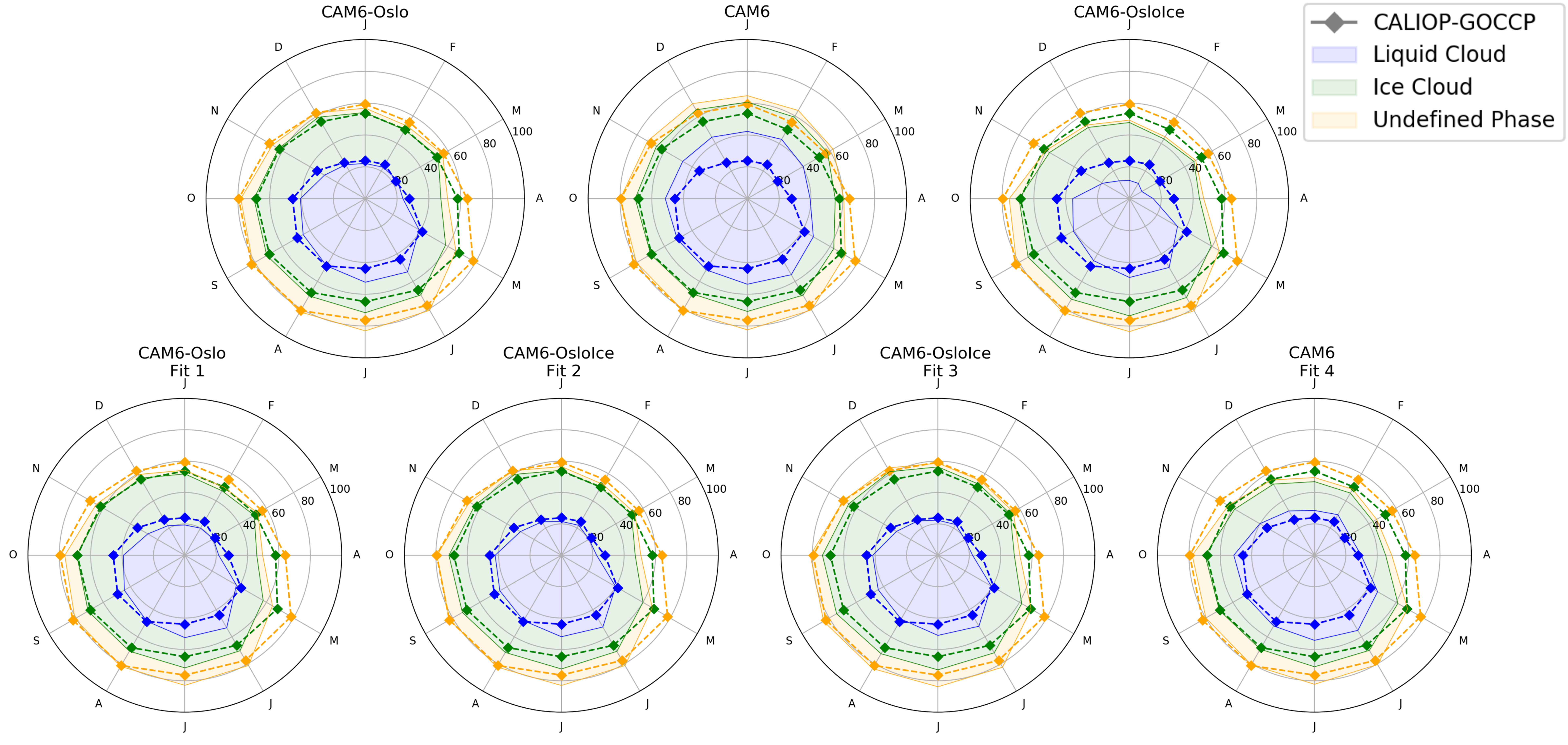

CAM6-Oslo
CAM6
CAM6-OsloIce
CALIOP-GOCCP
Liquid Cloud
Ice Cloud
Undefined Phase
CAM6-Oslo Fit 1
CAM6-OsloIce Fit 2
CAM6-OsloIce Fit 3
CAM6 Fit 4
J
F
M
A
M
J
J
A
S
O
N
D
20
40
60
80
100

Figure 3.

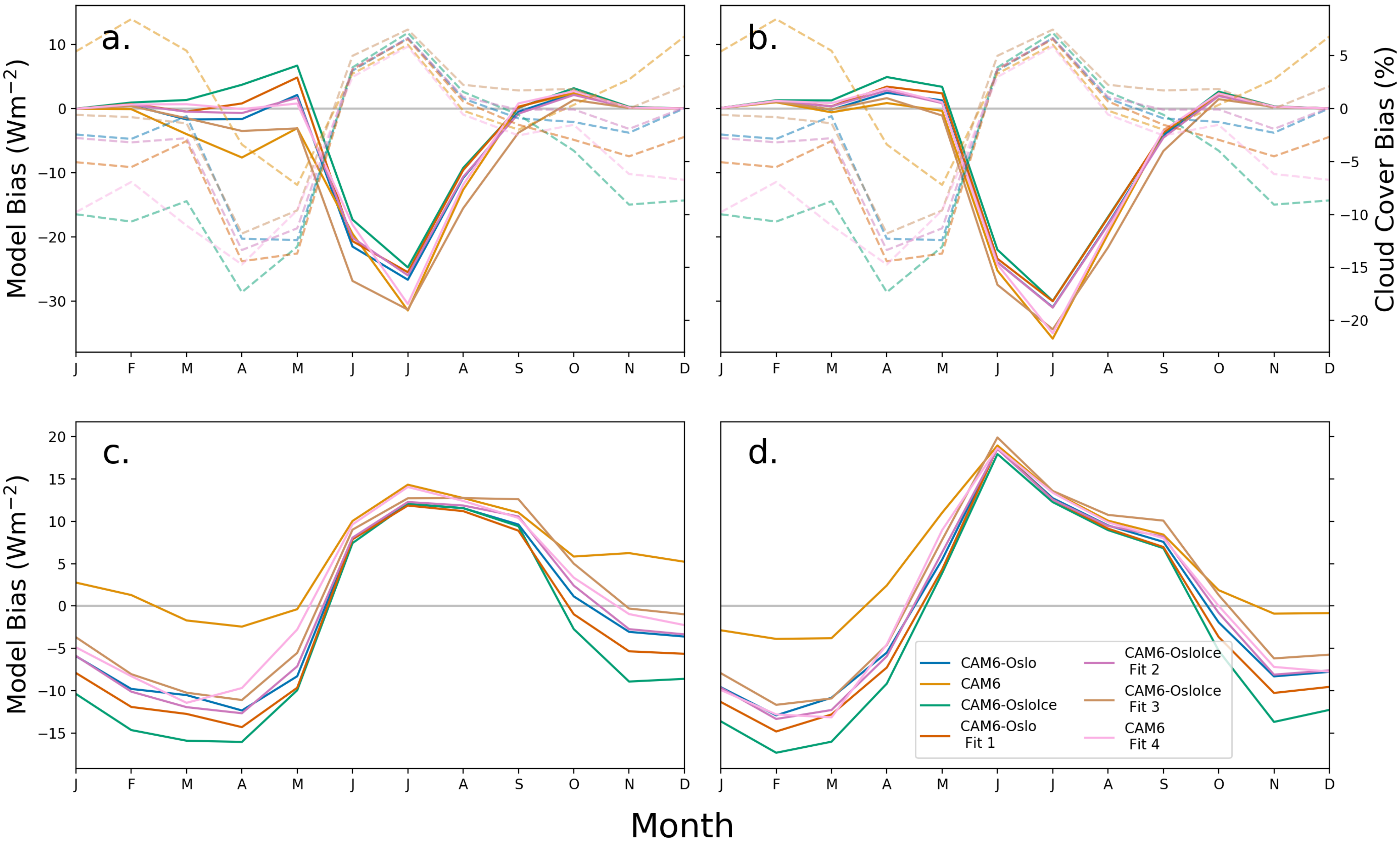
a.
b.
c.
d.
Model Bias (Wm^{-2})
Cloud Cover Bias (%)
J F M A M J J A S O N D
Month
CAM6-Oslo
CAM6
CAM6-OsloIce
CAM6-Oslo Fit 1
CAM6-OsloIce Fit 2
CAM6-OsloIce Fit 3
CAM6 Fit 4

Figure 4.

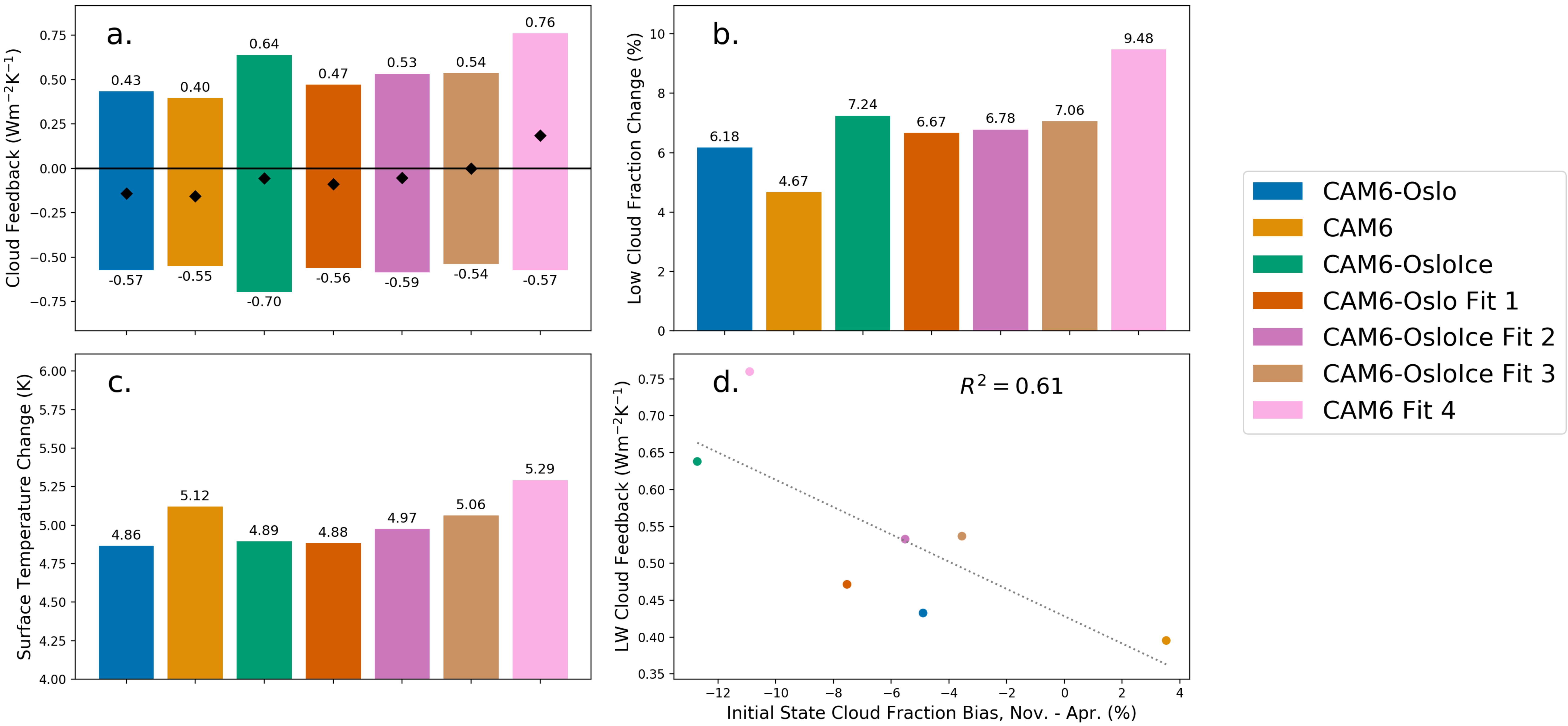

a.
Cloud Feedback (Wm^{-2}K^{-1})
0.43
0.40
0.64
0.47
0.53
0.54
0.76
-0.57
-0.55
-0.70
-0.56
-0.59
-0.54
-0.57
b.
Low Cloud Fraction Change (%)
6.18
4.67
7.24
6.67
6.78
7.06
9.48
c.
Surface Temperature Change (K)
4.86
5.12
4.89
4.88
4.97
5.06
5.29
d.
$R^2 = 0.61$
LW Cloud Feedback (Wm^{-2}K^{-1})
Initial State Cloud Fraction Bias, Nov. - Apr. (%)
CAM6-Oslo
CAM6
CAM6-OsloIce
CAM6-Oslo Fit 1
CAM6-OsloIce Fit 2
CAM6-OsloIce Fit 3
CAM6 Fit 4

Supporting Information for "Using satellite observations to evaluate model representation of Arctic mixed-phase clouds"

J. K. Shaw[1] *, Z. S. McGraw[1] †, O. Bruno[2], T. Storelvmo[1,3], and S. Hofer[1]

[1]Department of Geosciences, University of Oslo, Oslo, Norway

[2]Karlsruhe Institute of Technology, Institute of Meteorology and Climate Research

[3]School of Business, Nord University, Bodø, Norway

Contents of this file

1. Table S1
2. Figures S1 and S2

J. Shaw (jonah.shaw@colorado.edu)

*Now at Department of Atmospheric and Oceanic Sciences, University of Colorado, Boulder, Colorado, USA

†Now at Department of Applied Physics and Applied Mathematics, Columbia University

Run name	Total Cloud Bias (%)	Liquid Cloud Bias (%)	Ice Cloud Bias (%)	Undefined Cloud Bias (%)	Shortwave CRE Bias (W/m^2)	Longwave CRE Bias (W/m^2)
CAM6-Oslo	-2.0	-0.7	0.7	-1.8	-3.5	-0.1
CAM6	2.1	11.2	-7.9	-0.8	-4.0	-0.8
CAM6-OsloIce	-5.8	-8.2	6.1	-3.4	-2.9	0.3
CAM6-Oslo Fit 1	-3.6	-2.2	1.1	-2.2	-3.0	-0.6
CAM6-OsloIce Fit 2	-2.0	-0.9	1.6	-2.4	-3.7	0.4
CAM6-OsloIce Fit 3	-0.3	-1.3	3.6	-2.3	-5.1	1.8
CAM6 Fit 4	-5.1	5.4	-8.1	-2.0	-3.3	-1.9

Table S1. Annual model cloud biases for the region 66°N-82°N. Cloud cover biases are calculated relative to CALIOP GOCCP observations. Surface cloud radiative effect (CRE) biases are calculated relative to CERES-EBAF observations with a positive downward sign convention.

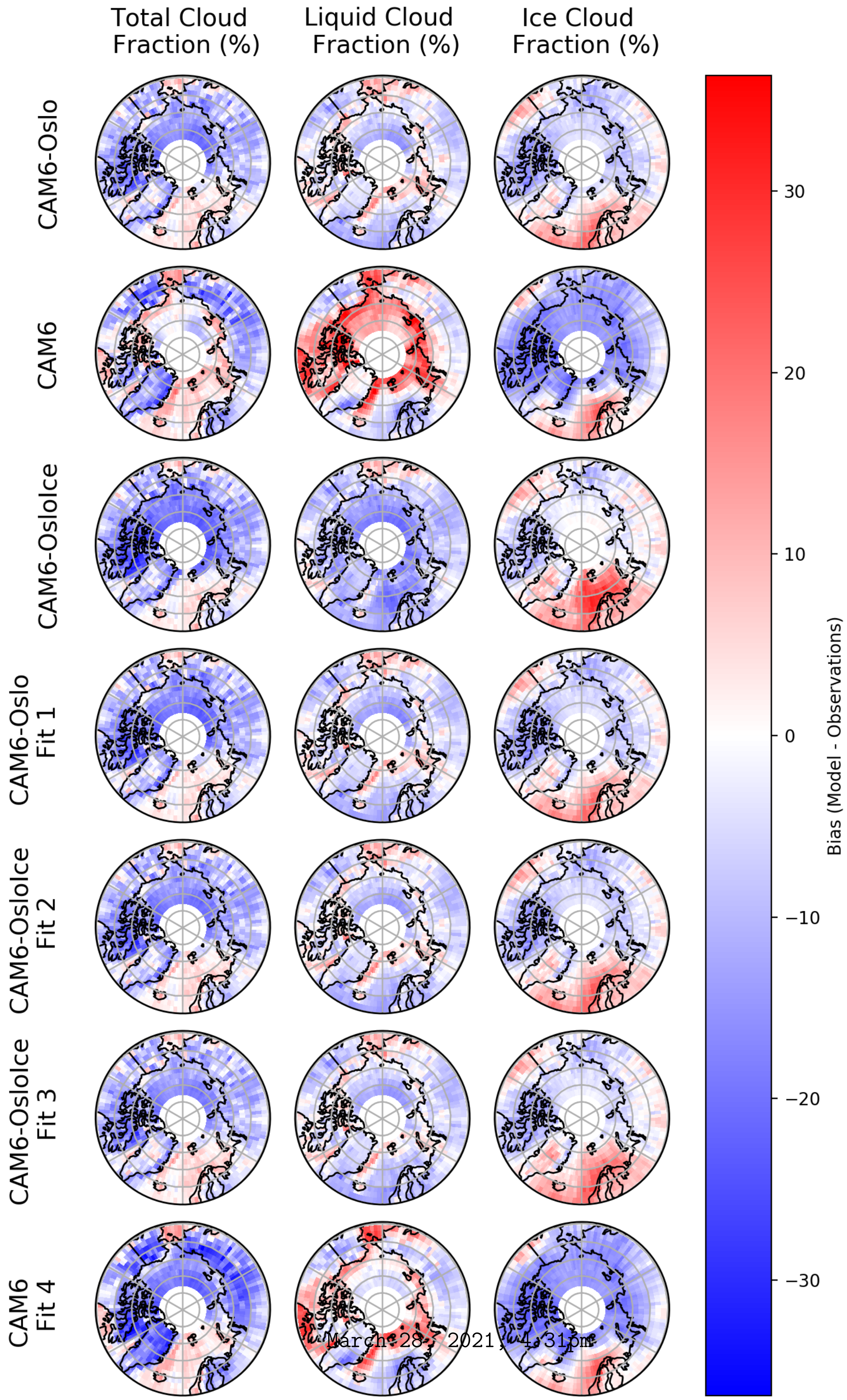

Figure S1. North Pole maps (60–90°N) of cloud cover bias by CALIOP phase designation.

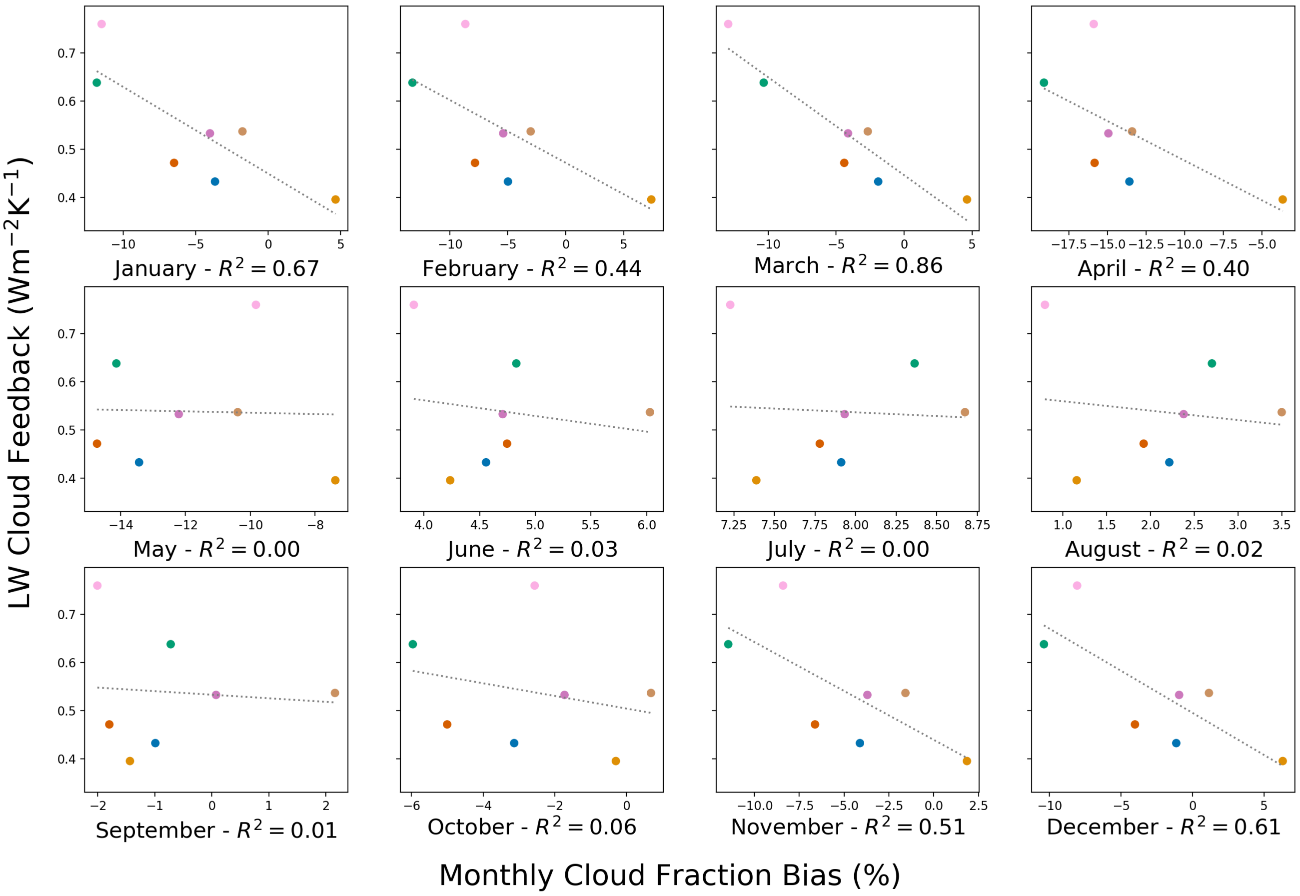

Figure S2. Longwave cloud feedback as a function of the average cloud cover by month in the simulated present-day.